Available online at www.sciencedirect.com
ScienceDirect
Journal of Sound and Vibration 299 (2007) 44–63
JOURNAL OF SOUND AND VIBRATION
www.elsevier.com/locate/jsvi

Free vibration behaviour of multiphase and layered magneto-electro-elastic beam

Anandkumar R. Annigeri, N. Ganesan, S. Swarnamani*

Machine Design Section, Mechanical Engineering Department, Indian Institute of Technology Madras, Chennai 600 036, India

Received 14 February 2006; received in revised form 6 June 2006; accepted 26 June 2006
Available online 22 August 2006

Abstract

Free vibration studies of multiphase and layered magneto-electro-elastic beam for $BaTiO_3$–$CoFe_2O_4$ composite is carried out. In-plane plate finite-element analysis is used to obtain the behaviour of magneto-electro-elastic beam. Studies are carried out for beams for different boundary conditions, as may be applicable in design of smart sensors/actuators. The ANSYS package is used to validate the results obtained by the computer code developed for piezoelectric (PE) beam. Plane stress condition is used for the Euler–Bernouli magneto-electro-elastic beam.

1. Introduction

Research on magneto-electro-elastic materials has gained considerable importance since the last decade. These smart composite materials exhibit a desirable coupling effect between electric and magnetic fields, which are useful in smart or intelligent structure applications. These materials have the capacity to convert one form of energy, viz., magnetic, electric and mechanical energy to another form of energy. The composites made of piezoelectric (PE) and piezomagnetic (PM) materials exhibit a magnetoelectric effect which is absent in single phase PE or PM materials [1]. The smart materials seem to provide unique capabilities of sensing and reacting to external disturbances, thus satisfying performance, reliability and light weight requirements imposed in any modern structural applications [2]. For smart structures, the two basic elements are actuators and sensors. Many materials are available for this purpose, but PE materials are used commonly due to the factors like capability to at either as actuator or sensor and directly relate electrical signals to material strains and vice versa. Composites consisting of PE and PM components have found increasing applications in engineering structures, particularly in smart materials/intelligent structure systems. Magneto-electro-elastic materials are extensively used as magnetic field probes, electric packaging, acoustic, hydrophones, medical ultrasonic imaging, sensors, and actuators with the responsibility of magneto-electro-mechanical energy conversion [3]. Pan [4] has derived exact solutions for three-dimensional (3-D), anisotropic, linearly magneto-electro-elastic, simply supported and multilayered rectangular plates under static loadings. The behaviour of finitely long cylindrical shells under pressure loading has been studied by Wang and Zhong [5]. Free vibration study of

*Corresponding author. Fax: +91 044 2350509.
E-mail address: mani46@iitm.ac.in (S. Swarnamani).

0022-460X/$ - see front matter © 2006 Elsevier Ltd. All rights reserved.
doi:10.1016/j.jsv.2006.06.044

simply supported and multilayered magneto-electro-elastic plates, has been carried out using propagator matrix approach, reported by Pan and Heyliger [6]. Buchanan [7] has studied the behaviour of infinitely long magneto-electro-elastic cylindrical shell using semi-analytical finite-element method. Annigeri et al. [8] have carried out a free vibration study of clamped–clamped magneto-electro-elastic cylindrical shell using semi-analytical finite-element method. Aboudi [9] has carried out micromechanical analysis of fully coupled electro-magneto-thermo-elastic composites. In his study, a homogenization micromechanical method is employed for the prediction of the effective moduli of magneto-electro-elastic composites. His study includes determination of effective elastic, PE, piezomagnetic, dielectric, magnetic permeability and electromagnetic coupling moduli, as well as effective thermal expansion coefficients and the associated pyroelectric and pyromagnetic constants for magneto-electro-elastic composite. Buchanan [10] has studied the vibration behaviour of an infinite plate consisting of layered versus multiphase magneto-electro-elastic composites. Recently, Jiang and Ding [11] have obtained analytical solutions to magneto-electro-elastic beams for different boundary conditions. Annigeri et al. [12] have carried out static study on magneto-electro-elastic beams for different boundary conditions using finite-element method. Annigeri et al. [13] have conducted free vibration studies on simply supported layered and multiphase magneto-electro-elastic cylindrical shells by semi-analytical finite-element method. Ramirez et al. [14] have analysed the free vibration response of two-dimensional (2-D) magneto-electro-elastic laminated plates. Ramirez et al. [15] have conducted a static analysis of functionally graded elastic anisotropic plates using a discrete layer approach Heyliger et al. [16] have studied the behaviour of 2-D static fields in magneto-electro-elastic laminates. From the literature survey, it is found that only few studies on free vibrations of magneto-electro-elastic beam structures have been reported.

Hence in the present paper, free vibration study of magneto-electro-elastic beam is carried out for three different boundary conditions, viz., clamped–clamped, clamped–free and simply supported ends. For the study, magneto-electro-elastic material $BaTiO_3$–$CoFe_2O_4$ composite is considered. The multiphase material properties vary and are dependant on the ratio of fiber material to matrix material for $BaTiO_3$–$CoFe_2O_4$ composite, the volume fraction of $BaTiO_3$ is increased in steps of 20% to obtain different multiphase beam configurations.

2. Constitutive relation

For an anisotropic and linearly magneto-electro-elastic solid the coupled constitutive relation [4] for a general three-dimensional solid is as follows:

$$\begin{Bmatrix}\sigma_1\\ \sigma_2\\ \sigma_3\\ \sigma_4\\ \sigma_5\\ \sigma_6\end{Bmatrix}=\begin{bmatrix}C_{11} & C_{12} & C_{13} & 0 & 0 & 0\\ C_{12} & C_{11} & C_{13} & 0 & 0 & 0\\ C_{13} & C_{13} & C_{33} & 0 & 0 & 0\\ 0 & 0 & 0 & C_{44} & 0 & 0\\ 0 & 0 & 0 & 0 & C_{44} & 0\\ 0 & 0 & 0 & 0 & 0 & C_{66}\end{bmatrix}\begin{Bmatrix}S_1\\ S_2\\ S_3\\ S_4\\ S_5\\ S_6\end{Bmatrix}-\begin{bmatrix}0 & 0 & e_{31}\\ 0 & 0 & e_{31}\\ 0 & 0 & e_{33}\\ 0 & e_{15} & 0\\ e_{15} & 0 & 0\\ 0 & 0 & 0\end{bmatrix}\begin{Bmatrix}E_1\\ E_2\\ E_3\end{Bmatrix}-\begin{bmatrix}0 & 0 & q_{31}\\ 0 & 0 & q_{31}\\ 0 & 0 & q_{33}\\ 0 & q_{15} & 0\\ q_{15} & 0 & 0\\ 0 & 0 & 0\end{bmatrix}\begin{Bmatrix}H_1\\ H_2\\ H_3\end{Bmatrix}, \tag{1}$$

$$\begin{Bmatrix}D_1\\ D_2\\ D_3\end{Bmatrix}=\begin{bmatrix}0 & 0 & 0 & 0 & e_{15} & 0\\ 0 & 0 & 0 & e_{15} & 0 & 0\\ e_{31} & e_{31} & e_{33} & 0 & 0 & 0\end{bmatrix}\begin{Bmatrix}S_1\\ S_2\\ S_3\\ S_4\\ S_5\\ S_6\end{Bmatrix}+\begin{bmatrix}\varepsilon_{11} & 0 & 0\\ 0 & \varepsilon_{11} & 0\\ 0 & 0 & \varepsilon_{33}\end{bmatrix}\begin{Bmatrix}E_1\\ E_2\\ E_3\end{Bmatrix}+\begin{bmatrix}m_{11} & 0 & 0\\ 0 & m_{11} & 0\\ 0 & 0 & m_{33}\end{bmatrix}\begin{Bmatrix}H_1\\ H_2\\ H_3\end{Bmatrix}, \tag{2}$$

$$\begin{Bmatrix} B_1 \\ B_2 \\ B_3 \end{Bmatrix} = \begin{bmatrix} 0 & 0 & 0 & 0 & q_{15} & 0 \\ 0 & 0 & 0 & q_{15} & 0 & 0 \\ q_{31} & q_{31} & q_{33} & 0 & 0 & 0 \end{bmatrix} \begin{Bmatrix} S_1 \\ S_2 \\ S_3 \\ S_4 \\ S_5 \\ S_6 \end{Bmatrix} + \begin{bmatrix} m_{11} & 0 & 0 \\ 0 & m_{11} & 0 \\ 0 & 0 & m_{33} \end{bmatrix} \begin{Bmatrix} E_1 \\ E_2 \\ E_3 \end{Bmatrix} + \begin{bmatrix} \mu_{11} & 0 & 0 \\ 0 & \mu_{11} & 0 \\ 0 & 0 & \mu_{33} \end{bmatrix} \begin{Bmatrix} H_1 \\ H_2 \\ H_3 \end{Bmatrix}, \tag{3}$$

where σ_j, D_j and B_j indicate the stress, electric displacement and magnetic induction. S_k, E_k and H_k are strain, electric field and magnetic field. c_{jk}, ε_{jk} and μ_{jk} are the elastic, dielectric and magnetic permeability coefficients, e_{kj}, q_{kj}, and m_{jk} are the piezo-electric, piezo-magnetic and magneto-electric material coefficients, respectively.

3. Finite-element formulations

For modeling of magneto-electro-elastic beam, four noded in-plane plate element with four degree of per node, i.e., displacement in axial direction (u), vertical direction (w), electric potential (ϕ) and magnetic potential (ψ) is used. Fig. 1 shows FE discretization using the in-plane plate elements.

The mechanical displacements, electrical potential and magnetic potential can be represented by suitable shape functions as follows:

$$u = [N_u]\{u\}, \quad \phi = [N_\psi]\{\phi\}, \quad \psi = [N_\psi]\{\psi\}. \tag{4}$$

Here N_u, N_ϕ and N_ψ are shape functions for structure, electric and magnetic field, respectively.

The dimensions of the beam are length $= 0.3$ m, height $h = 0.02$ m. For FE modeling of the beam 60 elements in X direction and four elements in the Z direction are used.

For plane stress problem, the stress components $\sigma_2(\sigma_{yy}) = \sigma_4(\sigma_{yz}) = \sigma_6$ $(\sigma_{xy}) = 0$, electric displacement component, D_2 $(D_y) = 0$, magnetic induction component are B_2 $(B_y) = 0$.

The strains for the 2-D element are:

$$S_1 = S_{xx} = \frac{\partial u}{\partial x}, \quad S_3 = S_{zz} = \frac{\partial w}{\partial z} \text{ and } S_5 = S_{zx} = \frac{\partial u}{\partial z} + \frac{\partial w}{\partial x}. \tag{5}$$

The electric field is related to electric potential as follows:

$$E_1 = -\frac{\partial \phi}{\partial x}, \quad E_3 = -\frac{\partial \phi}{\partial z}. \tag{6}$$

The magnetic field is related to magnetic potential as follows:

$$H_1 = -\frac{\partial \psi}{\partial x}, \quad H_3 = -\frac{\partial \psi}{\partial z}. \tag{7}$$

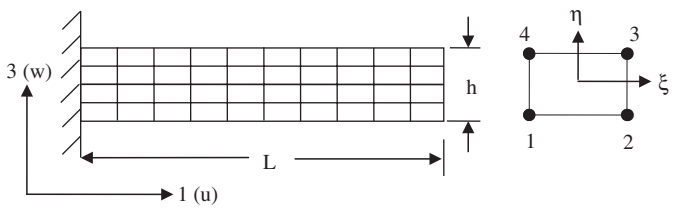

Fig. 1. FE discretization of cantilever beam.

The $[B_u]$ matrix for the plate element for strains is

$$[B_u] = [L_u][N_u] = \begin{bmatrix} \partial/\partial x & 0 \\ 0 & \partial/\partial z \\ \partial/\partial z & \partial/\partial x \end{bmatrix} \begin{bmatrix} N_1 & 0 & N_2 & 0 & N_3 & 0 & N_4 & 0 \\ 0 & N_1 & 0 & N_2 & 0 & N_3 & 0 & N_4 \end{bmatrix}. \tag{8}$$

The $[B_\phi]$ matrix for the plate element for electric field can be written as

$$\left[B_\phi\right] = \left[L_\phi\right]\left[N_\phi\right] = \begin{bmatrix} -\partial/\partial x \\ -\partial/\partial z \end{bmatrix} \begin{bmatrix} N_1 & N_2 & N_3 & N_4 \end{bmatrix}. \tag{9}$$

The $[B_\psi]$ matrix for the plate element for magnetic field is

$$\left[B_\psi\right] = \left[L_\psi\right]\left[N_\psi\right] = \begin{bmatrix} -\partial/\partial x \\ -\partial/\partial z \end{bmatrix} \begin{bmatrix} N_1 & N_2 & N_3 & N_4 \end{bmatrix}. \tag{10}$$

The thermodynamic potential for a 3-D magneto-electro-elastic solid is given by

$$G = G(S, E, H), \tag{11}$$

where S, E and H are independent variables which represent strain, electric field and magnetic field, respectively.

By using Eqs. (1)–(3) in Eq. (11), the variational expression for magneto-electro-elastic solid can be obtained as suggested by Soh and Liu [17] as follows:

$$G = \left(\frac{1}{2} S^{\mathrm{T}} C S\right) - \left(\frac{1}{2} E^{\mathrm{T}} \varepsilon E\right) - \left(\frac{1}{2} H^{\mathrm{T}} \mu H\right) - SeE - SqH - EmH, \tag{12}$$

where C, ε, μ represent elastic, dielectric and magnetic permeability coefficients and e, q, m indicate the PE, PM and magnetoelectric coefficients, respectively.

By minimizing Eq. (11) for nodal variables of shape functions for strain-displacement, electric field–electric potential, and magnetic field–magnetic potential, the finite-element equations for magneto-electro-elastic solid can be obtained. A FE formulation for such coupled field variables can be written as [10]

$$\left[[K_{uu}] - \omega^2[M]\right]\{u\} + \left[K_{u\phi}\right]\left\{\phi\right\} + \left[K_{u\psi}\right]\left\{\psi\right\} = 0, \tag{13}$$

$$\left[K_{u\phi}\right]^{\mathrm{T}}\{u\} - \left[K_{\phi\phi}\right]\left\{\phi\right\} - \left[K_{\phi\psi}\right]\left\{\psi\right\} = 0, \tag{14}$$

$$\left[K_{u\psi}\right]^{\mathrm{T}}\{u\} - \left[K_{\phi\psi}\right]^{\mathrm{T}}\left\{\phi\right\} - \left[K_{\psi\psi}\right]\left\{\psi\right\} = 0. \tag{15}$$

Different elemental stiffness matrices used for magneto-electro-elastic beam are as follows:

$$[K_{uu}] = \int_v [B_u]^{\mathrm{T}}[C][B_u]\,\mathrm{d}v, \tag{16}$$

$$\left[K_{u\psi}\right] = \int_v [B_u]^{\mathrm{T}}[q]\left[B_\psi\right]\,\mathrm{d}v, \tag{17}$$

$$\left[K_{u\phi}\right] = \int_v [B_u]^{\mathrm{T}}[e]\left[B_\phi\right]\,\mathrm{d}v, \tag{18}$$

$$\left[K_{\phi\psi}\right] = \int_v \left[B_\phi\right]^{\mathrm{T}}[m]\left[B_\psi\right]\,\mathrm{d}v, \tag{19}$$

$$\left[K_{\phi\phi}\right] = \int_v \left[B_\phi\right]^{\mathrm{T}}[\varepsilon]\left[B_\phi\right] \mathrm{d}v, \tag{20}$$

$$\left[K_{\psi\psi}\right] = \int_v \left[B_\psi\right]^{\mathrm{T}}[\mu]\left[B_\psi\right] \mathrm{d}v, \tag{21}$$

where $[B_u]$, $[B_\phi]$ and $[B_\psi]$ and are for strain-displacement, electric field–electric potential and magnetic field–magnetic potential, respectively.

Mass matrix for the structure is

$$[M] = \int_v [N]^{\mathrm{T}}[\rho][N] \mathrm{d}v. \tag{22}$$

By eliminating electric and magnetic potential terms by condensation technique, equivalent stiffness matrix $\left[K_{\mathrm{eq}}\right]$ is obtained as follows:

$$\left[K_{\mathrm{eq}}\right]\{u\} + [M]\{\ddot{u}\} = 0, \tag{23}$$

where

$$\left[K_{eq}\right] = [K_{uu}] + \left[K_{u\phi}\right][K_{II}]^{-1}[K_I] + \left[K_{u\psi}\right][K_{IV}]^{-1}[K_{III}]. \tag{24}$$

The component matrices for Eq. (24) are

$$[K_{\mathrm{I}}] = \left[K_{u\phi}\right]^{\mathrm{T}} - \left[K_{\phi\psi}\right]\left[K_{\psi\psi}\right]^{-1}\left[K_{u\psi}\right]^{\mathrm{T}}, \tag{25}$$

$$[K_{\mathrm{II}}] = \left[K_{\phi\phi}\right] - \left[K_{\phi\psi}\right]\left[K_{\psi\psi}\right]^{-1}\left[K_{\phi\psi}\right]^{\mathrm{T}}, \tag{26}$$

$$[K_{\mathrm{III}}] = \left[K_{u\psi}\right]^{\mathrm{T}} - \left[K_{\phi\psi}\right]^{\mathrm{T}}\left[K_{\phi\phi}\right]^{-1}\left[K_{u\phi}\right]^{\mathrm{T}}, \tag{27}$$

$$[K_{\mathrm{IV}}] = \left[K_{\psi\psi}\right] - \left[K_{\phi\psi}\right]^{\mathrm{T}}\left[K_{\phi\phi}\right]^{-1}\left[K_{\phi\psi}\right]. \tag{28}$$

The distribution of electric $\{\phi\}$ and magnetic $\{\psi\}$ potentials can be as follows:

$$\phi = [K_{\mathrm{II}}]^{-1}[K_{\mathrm{I}}]\{u\}, \tag{29}$$

$$\psi = [K_{\mathrm{IV}}]^{-1}[K_{\mathrm{III}}]\{u\}. \tag{30}$$

To study the effect of magnetoelectric constant (m) on the system frequencies, equivalent stiffness matrix $[K_{\mathrm{eq\_reduced}}]$ is derived by neglecting the coupling between PE $BaTiO_3$ and PM $CoFe_2O_4$ materials. The magnetoelectric material coefficient (m) is zero for single phase $BaTiO_3$ and $CoFe_2O_4$ [10].

By making $\left[K_{\phi\psi}\right] = 0$, the reduced FE equations are as follows.

$$\left[[K_{uu}] - \omega^2[M]\right]\{u\} + \left[K_{u\phi}\right]\{\phi\} + \left[K_{u\psi}\right]\{\psi\} = 0,$$

$$\left[K_{u\phi}\right]^{\mathrm{T}}\{u\} - \left[K_{\phi\phi}\right]\{\phi\} = 0, \tag{31}$$

$$\left[K_{u\psi}\right]^{\mathrm{T}}\{u\} - \left[K_{\psi\psi}\right]\{\psi\} = 0.$$

The reduced stiffness matrix $[K_{\mathrm{eq\_reduced}}]$ is

$$\left[K_{\mathrm{eq\_reduced}}\right] = [K_{uu}] + \left[K_{u\phi}\right]\left[K_{\phi\phi}\right]^{-1}\left[K_{u\phi}\right]^{\mathrm{T}} + \left[K_{u\psi}\right]\left[K_{\psi\psi}\right]^{-1}\left[K_{u\psi}\right]^{\mathrm{T}}. \tag{32}$$

Table 1
List of $[K_{eq}]$ matrices used in the study

Symbol	Description
$\left[K_{eq}\right]$	Stiffness matrix for fully coupled magneto-electro-elastic material
$\left[K_{eq\_reduced}\right]$	Stiffness matrix neglecting magneto-electric coupling
$\left[K_{eq\_\phi\phi}\right]$	Stiffness matrix considering piezoelectric effect
$\left[K_{eq\_\psi\psi}\right]$	Stiffness matrix considering piezomagnetic effect

To study the effect of PE phase on frequency of beam, the stiffness matrix $\left[K_{eq\_\phi\phi}\right]$ is derived by putting magnetic potential to zero as follows:

$$\left[K_{eq\_\phi\phi}\right] = [K_{uu}] + \left[K_{u\phi}\right]\left[K_{\phi\phi}\right]^{-1}\left[K_{u\phi}\right]^{T}. \tag{33}$$

To study the magnetic effect of PM phase on frequency of the system, the matrix $\left[K_{eq\_\psi\psi}\right]$ is obtained by putting electric potential to zero in Eqs. (13)–(15)

$$\left[K_{eq\_\psi\psi}\right] = [K_{uu}] + \left[K_{u\psi}\right]\left[K_{\psi\psi}\right]^{-1}\left[K_{u\psi}\right]^{T}. \tag{34}$$

Table 1 gives in brief the various stiffness matrices used in the study of free vibrations of magneto-electro-elastic beam.

The matrices of magneto-electro-elastic material constants $[C]$, $[\varepsilon]$, $[\mu]$, $[e]$, $[q]$ and $[m]$ are derived for beam are as given below [11].

The elastic constants $[C]$ matrix is defined for plane stress case is

$$[C] = \begin{bmatrix} \overline{C}_{11} & \overline{C}_{13} & 0 \\ \overline{C}_{13} & \overline{C}_{33} & 0 \\ 0 & 0 & \overline{C}_{44} \end{bmatrix}, \tag{35}$$

where

$$\overline{C}_{11} = \left(\frac{C_{11}^2 - C_{12}^2}{C_{11}}\right), \quad \overline{C}_{13} = \left(\frac{(C_{11} - C_{12})C_{13}}{C_{11}}\right), \quad \overline{C}_{33} = \left(\frac{C_{11}C_{33} - C_{13}^2}{C_{11}}\right), \quad \overline{C}_{44} = C_{44}. \tag{36}$$

The magnetic permeability matrix is

$$[\mu] = \begin{bmatrix} \overline{\mu}_{11} & 0 \\ 0 & \overline{\mu}_{33} \end{bmatrix}, \tag{37}$$

where

$$\overline{\mu}_{11} = \mu_{11}, \quad \overline{\mu}_{33} = \left(\frac{C_{11}\mu_{33} + q_{31}^2}{C_{11}}\right). \tag{38}$$

The dielectric coefficient matrix for the magneto-electro-elastic beam is

$$[\varepsilon] = \begin{bmatrix} \overline{\varepsilon}_{11} & 0 \\ 0 & \overline{\varepsilon}_{33} \end{bmatrix}, \tag{39}$$

where

$$\overline{\varepsilon}_{11} = \varepsilon_{11}, \quad \overline{\varepsilon}_{33} = \left(\frac{C_{11}C_{33} + e_{31}^2}{C_{11}}\right). \tag{40}$$

The PM coefficient matrix

$$[q] = \begin{Bmatrix} 0 & \overline{q}_{31} \\ 0 & \overline{q}_{33} \\ \overline{q}_{15} & 0 \end{Bmatrix}, \tag{41}$$

where

$$\overline{q}_{31} = \left(\frac{(C_{11} - C_{12})q_{31}}{C_{11}}\right), \quad \overline{q}_{33} = \left(\frac{C_{11}q_{33} - C_{13}q_{31}}{C_{11}}\right), \quad \overline{q}_{15} = q_{15}. \tag{42}$$

The PE coefficient matrix is

$$[e] = \begin{Bmatrix} 0 & \overline{e}_{31} \\ 0 & \overline{e}_{33} \\ \overline{e}_{15} & 0 \end{Bmatrix}, \tag{43}$$

where

$$\overline{e}_{31} = \left(\frac{(C_{11} - C_{12})e_{31}}{C_{11}}\right), \quad \overline{e}_{33} = \left(\frac{C_{11}e_{33} - C_{13}e_{31}}{C_{11}}\right), \quad \overline{e}_{15} = e_{15}. \tag{44}$$

The magneto-electric coefficients matrix is as follows:

$$[m] = \begin{bmatrix} \overline{m}_{11} & 0 \\ 0 & \overline{m}_{33} \end{bmatrix}, \tag{45}$$

where

$$\overline{m}_{11} = m_{11}, \quad \overline{m}_{33} = \left(\frac{C_{11}m_{33} + e_{31}q_{31}}{C_{11}}\right). \tag{46}$$

4. Results and discussion

4.1. Validation

The computer programme developed is validated with ANSYS results for eigenfrequencies, by treating the beam made of PE material (vf = 100% of $BaTiO_3$). The three boundary conditions, viz., clamped–free (C–F), simply supported (S–S) and clamped–clamped (C–C) beams with plane stress case are considered for the study. The *Plane13* element with plane stress condition is used in conjunction with coupled field analysis in ANSYS® multiphysics. Here [*C*], [*e*] and [ε] material properties are used in the PE beam model, as magneto-electro-elastic modeling is not available in ANSYS. For modeling of the beam, 60 elements along axial direction and four elements along thickness direction are used. Tables 2–4 show the first five modes of frequencies for the three boundary conditions. ANSYS results for three different meshes 4×60, 8×120 and 16×240 for purely PE $BaTiO_3$ beam are tabulated for C–F, C–C and S–S boundary conditions. Good match of frequencies with the present computer code is noticed. By observing the ANSYS results for different meshes for each of the boundary conditions, 4×60 mesh is selected for the study of free vibrations of magneto-electro-elastic beam.

4.2. Multiphase beams

The free vibration studies on magneto-electro-elastic beams are carried out by changing the volume fraction (vf) of $BaTiO_3$ in composite of $BaTiO_3$–$CoFe_2O_4$. The dimensions of the beam are $L = 0.3$ m and $h = 0.02$ m with plane stress assumption. The number of finite elements used are 60 in axial direction and four in thickness

Table 2
Frequencies (in Hz) for clamped-free beam vf = 100% of $BaTiO_3$

Mode	ANSYS			Present study
	60×4	120×8	240×16	
1	170.98	170.88	170.83	167.17
2	1049.70	1048.10	1047.50	1029.73
3	2850.50	2841.80	2839.20	2809.58
4	3982.30	3981.30	3980.90	3841.22
5	5363.50	5336.30	5328.70	5317.97

Table 3
Frequencies (in Hz) for simply supported end beam vf = 100% of $BaTiO_3$

Mode	ANSYS			Present study
	60×4	120×8	240×16	
1	476.88	476.58	476.43	467.38
2	1866.50	1862.10	1859.90	1835.70
3	3673.00	3580.10	3490.60	3573.48
4	4061.40	4041.20	4031.00	4014.79
5	6921.60	6864.80	6836.40	6883.36

Table 4
Frequencies (in Hz) for clamped–clamped beam vf = 100% of $BaTiO_3$

Mode	ANSYS			Present study
	60×4	120×8	240×16	
1	1061.90	1059.30	1058.40	1042.34
2	2822.60	2810.70	2807.00	2783.21
3	5295.50	5262.10	5252.30	5267.51
4	7981.30	7976.80	7975.10	7689.42
5	8330.80	8258.70	8238.40	8333.28

direction of the beam. The density of the PE $BaTiO_3$ and PM $CoFe_2O_4$ is assumed to be same. The study is conducted by choosing six different beams with volume fractions (vf) of $BaTiO_3$ in steps of 20%, i.e., 0%, 20%, 40%, 60%, 80% and 100%. The magneto-electro-elastic properties are listed in Table 5, with different volume fraction (vf) of $BaTiO_3$ in composite of $BaTiO_3$–$CoFe_2O_4$, after obtaining them by scaling from the graphical results given by Aboudi [9].

The following notations are used in subsequent discussions of free vibration of magneto-electro-elastic beam. The frequency is given in Hertz.

f_{uu} Structural frequency computed by using $[K_{uu}]$ and shows only effect of elastic constants on beam frequencies. f_{eq} is System frequency computed by using $[K_{eq}]$ and shows the coupled field effect on beam frequency. $f_{eq\_reduced}$ is System frequency computed by using $[K_{eq\_reduced}]$ and indicates the effect of magnetoelectric coupling effect when compared with f_{eq} values; $f_{\psi\psi}$ is System frequency computed by using $[K_{\psi\psi}]$ and shows the effect of PM phase. $f_{\phi\phi}$ is system frequency computed by using $[K_{\phi\phi}]$ and indicates the effect of PE phase on beam frequencies.

4.2.1. C–F beam

Boundary conditions used for the study of multiphase magneto-electro-elastic beam are $u = w = \psi = \phi = 0$ at the clamped end. Tables 6–8 show the free vibration behaviour for vf = 0%, 60% and 100% vf of $BaTiO_3$,

Table 5
Material constants for MEE $BaTiO_3$–$CoFe_2O_4$ composite [9]

vf	0%	20%	40%	60%	80%	100%
C_{11}	286	250	225	200	175	166
C_{12}	173	146	125	110	100	77
C_{13}	170	145	125	110	100	78
C_{33}	269.5	240	220	190	170	162
C_{44}	45.3	45	45	45	50	43
e_{31}	0	−2	−3	−3.5	−4	−4.4
e_{33}	0	4	7	11	14	18.6
e_{15}	0	0	0	0	0	11.6
ε_{11}	0.08	0.33	0.8	0.9	1.0	11.2
ε_{33}	0.093	2.5	5.0	7.5	10	12.6
μ_{11}	−5.9	−3.9	−2.5	−1.5	−0.8	0.05
μ_{33}	1.57	1.33	1.0	0.75	0.5	0.1
q_{31}	580	410	300	200	100	0
q_{33}	700	550	380	260	120	0
q_{15}	560	340	220	180	80	0
m_{11}	0	2.8	4.8	6.0	6.8	0
m_{33}	0	2000	2750	2500	1500	0

C_{ij} in $10^9\,N/m^2$, e_{ij} in C/m^2, ε_{ij} in $10^{-9}\,C/V\,m$, q_{ij} in $N/A\,m$, μ_{ij} in $10^{-4}\,N\,s^2/C^2$ and m_{ij} in $10^{-12}\,N\,s/VC$.

Table 6
Frequencies in Hz for clamped-free beam vf = 0% of $BaTiO_3$

No.	f_{uu}	$f_{k_{eq}}$	$f_{k_{eq\_reduced}}$	$f_{\psi\psi}$	$f_{\phi\phi}$
1	188.68	188.70	188.70	188.70	188.68
2	1154.77	1154.65	1154.65	1154.65	1154.77
3	3122.08	3120.80	3120.80	3120.80	3122.08
4	4334.45	4335.11	4335.11	4335.11	4334.45
5	5842.88	5838.36	5838.36	5838.36	5842.88
6	9165.19	9154.66	9154.66	9154.66	9165.19
7	12944.51	12924.91	12924.91	12924.91	12944.51
8	12999.53	13001.48	13001.48	13001.48	12999.53
9	17068.11	17036.45	17036.45	17036.45	17068.11
10	21451.57	21405.15	21405.15	21405.15	21451.57

in $BaTiO_3$–$CoFe_2O_4$ composite. Table 6 shows the free vibration behaviour of vf = 0% $BaTiO_3$, which is purely a PM $CoFe_2O_4$, its influence on frequency of the structure due to magnetic effect is marginally higher when compared with the conventional structural frequency of beam. The $f_{\phi\phi}$ coincides with the structural frequency since PE phase is absent for vf = 0% $BaTiO_3$. Similarly $f_{eq\_reduced}$ frequencies coincide with f_{eq} of the beam as the magnetoelectric effect is absent in pure $CoFe_2O_4$ beam. Table 7 shows the free vibration behaviour of vf = 60% $BaTiO_3$,

Table 8 shows the free vibration behaviour of vf = 100% $BaTiO_3$, which is purely a PE $BaTiO_3$ its influence on frequency of the structure due to PE phase in the composite is higher when compared with the f_{uu} of beam. The $f_{\phi\phi}$ coincides with the $f_{k_{eq}}$ since PM phase is absent for vf = 100% $BaTiO_3$. Similarly $f_{eq\_reduced}$ frequencies coincide with f_{eq} of the beam as the magnetoelectric effect is absent in pure $BaTiO_3$ beam. It can be observed that by increasing the volume fraction of $BaTiO_3$ in $BaTiO_3$–$CoFe_2O_4$ composite, the frequency of the system decreases and this may be due to decreasing value of elastic constants [*C*] and this decreases the stiffness of the clamped-free beam.

Table 7
Frequencies in Hz for clamped-free beam vf = 60% of $BaTiO_3$

Mode	f_{uu}	$f_{k_{eq}}$	$f_{k_{eq\_reduced}}$	$f_{\psi\psi}$	$f_{\phi\phi}$
1	167.08	169.97	169.97	167.09	169.96
2	1026.71	1043.76	1043.77	1026.68	1043.76
3	2791.80	2835.36	2835.37	2791.45	2835.65
4	3828.24	3902.01	3902.02	3828.46	3901.62
5	5261.76	5337.23	5337.24	5260.46	5338.44
6	8315.01	8423.05	8423.06	8311.87	8426.11
7	11481.88	11704.94	11704.98	11482.54	11703.78
8	11829.32	11967.14	11967.17	11823.31	11973.11
9	15704.50	15867.42	15867.44	15694.58	15877.37
10	19126.55	19504.23	19504.30	19127.60	19502.35

Table 8
Frequencies in Hz for clamped–free beam vf = 100% of $BaTiO_3$

Mode	f_{uu}	$f_{k_{eq}}$	$f_{k_{eq\_reduced}}$	$f_{\psi\psi}$	$f_{\phi\phi}$
1	163.84	167.17	167.17	163.84	167.17
2	1006.65	1029.73	1029.73	1006.65	1029.73
3	2736.64	2809.58	2809.58	2736.64	2809.58
4	3758.91	3841.22	3841.22	3758.91	3841.22
5	5156.31	5317.97	5317.97	5156.31	5317.97
6	8145.80	8442.61	8442.61	8145.80	8442.61
7	11275.21	11522.79	11522.79	11275.21	11522.79
8	11584.91	12066.57	12066.57	11584.91	12066.57
9	15375.32	16091.16	16091.16	15375.32	16091.16
10	18786.65	19201.57	19201.57	18786.65	19201.57

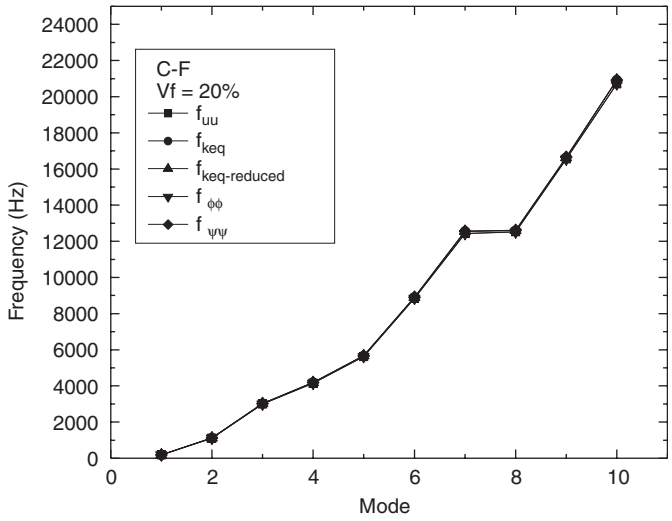

Fig. 2. Free vibrations of clamped–free multiphase MEE beam with vf = 20% $BaTiO_3$.

Figs. 2–4 show the free vibration behaviour for vf = 20%, 40% and 80% vf of $BaTiO_3$, in $BaTiO_3$–$CoFe_2O_4$ composite for clamped free beam. Fig. 2 shows the free vibration behaviour of vf = 20% $BaTiO_3$ beam, which consists 80% PM $CoFe_2O_4$, its influence on frequency of the structure due to magnetic effect is marginally

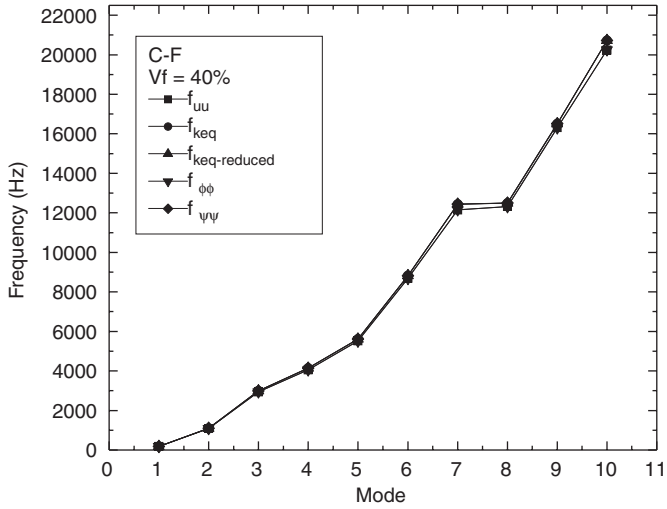

Fig. 3. Free vibrations of clamped–free multiphase MEE beam with vf = 40% $BaTiO_3$.

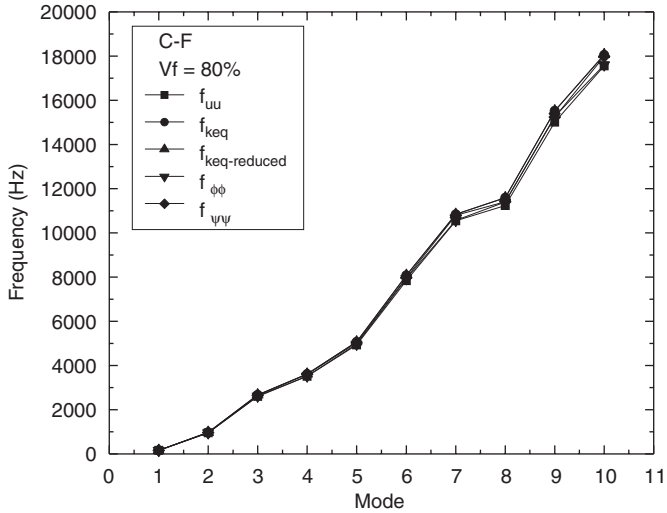

Fig. 4. Free vibrations of clamped–free multiphase MEE beam with vf = 80% $BaTiO_3$.

higher when compared with the conventional structural frequency of beam. The graph of $f_{\phi\phi}$ coincides with the $f_{k_{eq}}$ graph. The difference in frequency of $f_{eq\_reduced}$ and system frequency f_{eq} of is marginal in beam as the magnetoelectric effect is very low. For modes 7 and 8 the frequency of beam is almost same.

Fig. 3 shows the free vibration behaviour of vf = 40% $BaTiO_3$ beam, which consists 60% PM $CoFe_2O_4$, its influence on frequency of the structure due to magnetic effect is marginally higher when compared with the conventional structural frequency of beam. The graphs of $f_{\phi\phi}$ coincides with the $f_{k_{eq}}$ graph. At higher modes the marginal coupling effect is visible for vf = 40% plot.

Fig. 4 shows the free vibration behaviour of vf = 80% $BaTiO_3$ beam, which consists 20% PM $CoFe_2O_4$, its influence on frequency of the structure due to magnetic effect is marginally higher when compared with the conventional structural frequency of beam from the third mode onwards the magneto-electric coupling effect is felt on the frequency.

4.2.2. S–S beam

Tables 9–11 show the free vibration study of vf = 0%, 60% and 100% of $BaTiO_3$, in $BaTiO_3$–$CoFe_2O_4$ composite beam for simply supported boundary conditions. Boundary conditions used for the study of

Table 9
Frequencies in Hz for simply supported beam vf = 0% of $BaTiO_3$

Mode	f_{uu}	$f_{k_{eq}}$	$f_{k_{eq\_reduced}}$	$f_{\psi\psi}$	$f_{\phi\phi}$
1	526.26	526.29	526.29	526.29	526.26
2	2053.13	2052.71	2052.71	2052.71	2053.13
3	4010.34	4008.32	4008.32	4008.32	4010.34
4	4446.48	4444.36	4444.36	4444.36	4446.48
5	7536.74	7529.14	7529.14	7529.14	7536.74
6	11159.96	11146.34	11146.34	11146.34	11159.96
7	12057.90	12053.32	12053.32	12053.32	12057.90
8	15178.78	15150.08	15150.08	15150.08	15178.78
9	19487.01	19449.43	19449.43	19449.43	19487.01
10	20171.47	20163.37	20163.37	20163.37	20171.47

Table 10
Frequencies in Hz for simply supported beam vf = 60% of $BaTiO_3$

Mode	f_{uu}	$f_{k_{eq}}$	$f_{k_{eq\_reduced}}$	$f_{\psi\psi}$	$f_{\phi\phi}$
1	466.41	474.67	474.68	466.42	474.64
2	1827.29	1858.33	1858.33	1827.21	1858.36
3	3567.74	3632.54	3632.55	3567.74	3632.45
4	3981.49	4045.01	4045.02	3981.02	4045.42
5	6796.48	6896.23	6896.25	6794.58	6898.03
6	10138.17	10274.55	10274.56	10134.76	10277.98
7	10721.19	10918.21	10918.24	10721.19	10917.90
8	13888.65	14056.89	14056.92	13881.05	14064.45
9	17919.90	18150.64	18150.66	17920.09	18160.85
10	17952.17	18256.71	18256.77	17942.37	18255.91

Table 11
Frequencies in Hz for simply supported beam vf = 100% of $BaTiO_3$

Mode	f_{uu}	$f_{k_{eq}}$	$f_{k_{eq\_reduced}}$	$f_{\psi\psi}$	$f_{\phi\phi}$
1	457.53	467.38	467.38	457.53	467.38
2	1792.13	1835.70	1835.70	1792.13	1835.70
3	3501.34	3573.49	3573.49	3501.34	3573.49
4	3903.75	4014.80	4014.80	3903.75	4014.80
5	6661.47	6883.37	6883.37	6661.47	6883.37
6	9933.18	10317.11	10317.11	9933.18	10317.11
7	10523.04	10741.95	10741.95	10523.04	10741.95
8	13602.95	14199.70	14199.70	13602.95	14199.70
9	17576.92	17965.28	17965.28	17576.92	17965.28
10	17593.26	18441.67	18441.67	17593.26	18441.67

multiphase magneto-electro-elastic beam are $u = w = \psi = \phi = 0$ at $(x = 0,\ z = h/2)$ and $w = \psi = \phi = 0$ at $(x = L,\ z = h/2)$. Table 9 shows the free vibration behaviour of vf = 0% $BaTiO_3$, which is purely a PM $CoFe_2O_4$, its influence on frequency of the structure due to magnetic effect is marginally higher when

compared with the conventional structural frequency of beam. The $f_{\phi\phi}$ coincides with the structural frequency as the PE phase is absent for vf = 0% $BaTiO_3$. Similarly $f_{\text{eq\_reduced}}$ frequencies coincide with f_{eq} of the beam as the magnetoelectric effect is absent in single phase beam.

Table 11 shows the free vibration frequencies of vf = 100% $BaTiO_3$, which is purely a PE $BaTiO_3$. The purely PE phase in the composite increases the system frequency of beam $f_{k_{\text{eq}}}$ it can be observed by comparing frequency f_{uu} of beam. The $f_{\phi\phi}$ coincides with the $f_{k_{\text{eq}}}$ since PM phase is absent for vf = 100% $BaTiO_3$. Similarly $f_{\text{eq\_reduced}}$ frequencies coincide with f_{eq} of the beam as the magnetoelectric effect is absent in pure $BaTiO_3$ beam. It can be observed here that by increasing the volume fraction of $BaTiO_3$ in $BaTiO_3$–$CoFe_2O_4$ composite, the frequency of the system decreases, which may be due to decreasing value of elastic constants [C] and this decreases the stiffness of the clamped-free beam. The influence of PE and PM phase effect is more in simply supported beams as compared to clamped-free beams.

Figs. 5–7 show the free vibration behaviour for vf = 20%, 40% and 80% vf of $BaTiO_3$, in $BaTiO_3$–$CoFe_2O_4$ composite for simply supported beam. Fig. 5 shows the free vibration behaviour of vf = 20% $BaTiO_3$ beam,

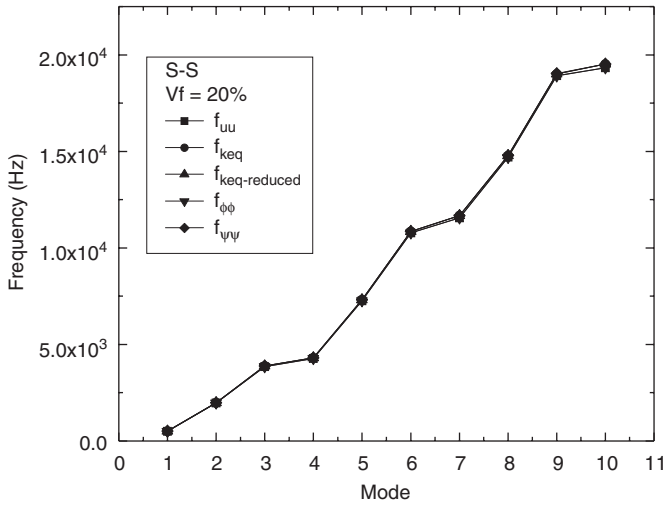

Fig. 5. Free vibrations of simply supported multiphase MEE beam with vf = 20% $BaTiO_3$.

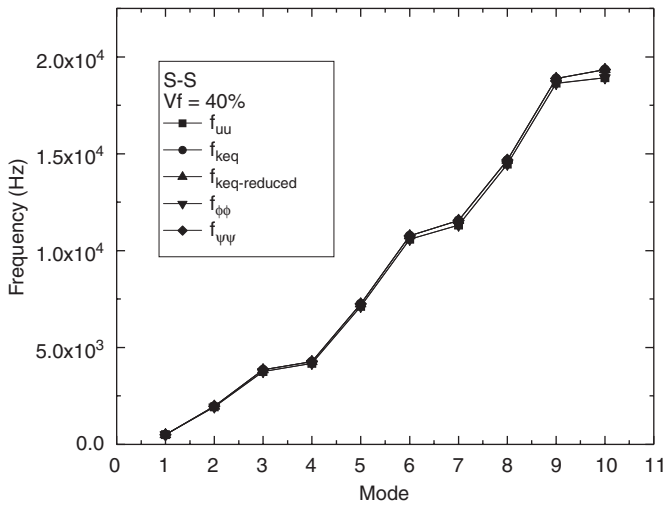

Fig. 6. Free vibrations of simply supported multiphase MEE beam with vf = 40% $BaTiO_3$.

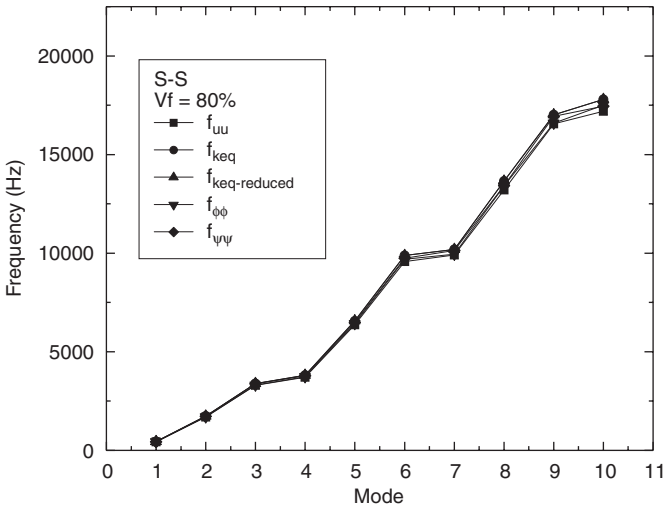

Fig. 7. Free vibrations of simply supported multiphase MEE beam with vf = 80% $BaTiO_3$.

Table 12
Frequencies in Hz for clamped–clamped beam vf = 0% of $BaTiO_3$

Mode	f_{uu}	$f_{k_{eq}}$	$f_{k_{eq\_reduced}}$	$f_{\psi\psi}$	$f_{\phi\phi}$
1	1165.34	1165.07	1165.07	1165.07	1165.34
2	3080.27	3078.60	3078.60	3078.60	3080.27
3	5744.55	5738.67	5738.67	5738.67	5744.55
4	8682.03	8683.41	8683.41	8683.41	8682.03
5	8983.76	8971.57	8971.57	8971.57	8983.76
6	12663.10	12640.40	12640.40	12640.40	12663.10
7	16677.80	16643.20	16643.20	16643.20	16677.80
8	17356.70	17358.00	17358.00	17358.00	17356.70
9	20951.10	20900.40	20900.40	20900.40	20951.10
10	25427.30	25360.00	25360.00	25360.00	25427.30

Table 13
Frequencies in Hz for clamped–clamped beam vf = 60% of $BaTiO_3$

Mode	f_{uu}	$f_{k_{eq}}$	$f_{k_{eq\_reduced}}$	$F_{\psi\psi}$	$f_{\phi\phi}$
1	1038.54	1054.93	1054.93	1038.49	1054.95
2	2765.50	2805.75	2805.75	2765.05	2806.12
3	5198.55	5266.99	5267.00	5196.90	5268.60
4	7668.05	7812.88	7812.91	7668.45	7812.12
5	8194.56	8291.21	8291.22	8190.88	8294.81
6	11637.00	11758.60	11758.60	11630.00	11765.60
7	15330.70	15572.90	15573.00	15331.50	15584.00
8	15430.40	15623.80	15623.80	15419.30	15622.20
9	19501.50	19659.70	19659.80	19485.00	19676.40
10	22981.50	23430.00	23430.00	22982.70	23427.70

which consists 80% PM $CoFe_2O_4$, its influence on frequency of the structure due to magnetic effect is marginally higher when compared with the conventional structural frequency of beam. The graph of $f_{\phi\phi}$ coincides with the $f_{k_{eq}}$ graph.

Table 14
Frequencies in Hz for clamped–clamped beam vf = 100% of $BaTiO_3$

Mode	f_{uu}	$f_{k_{eq}}$	$f_{k_{eq\_reduced}}$	$f_{\psi\psi}$	$f_{\phi\phi}$
1	1017.78	1042.34	1042.34	1017.78	1042.34
2	2709.55	2783.21	2783.21	2709.55	2783.21
3	5091.96	5267.51	5267.51	5091.96	5267.51
4	7526.76	7689.42	7689.42	7526.76	7689.42
5	8024.23	8333.28	8333.28	8024.23	8333.28
6	11391.90	11911.30	11911.30	11391.90	11911.30
7	15050.70	15377.10	15377.10	15050.70	15377.10
8	15101.50	15847.90	15847.90	15101.50	15847.90
9	19081.20	20140.20	20140.20	19081.20	20140.20
10	22568.30	23060.80	23060.80	22568.30	23060.80

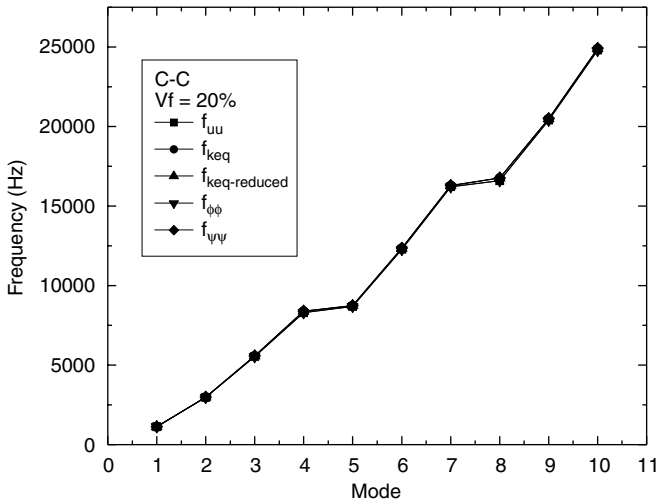

Fig. 8. Free vibrations of clamped–clamped multiphase MEE beam with vf = 20% $BaTiO_3$.

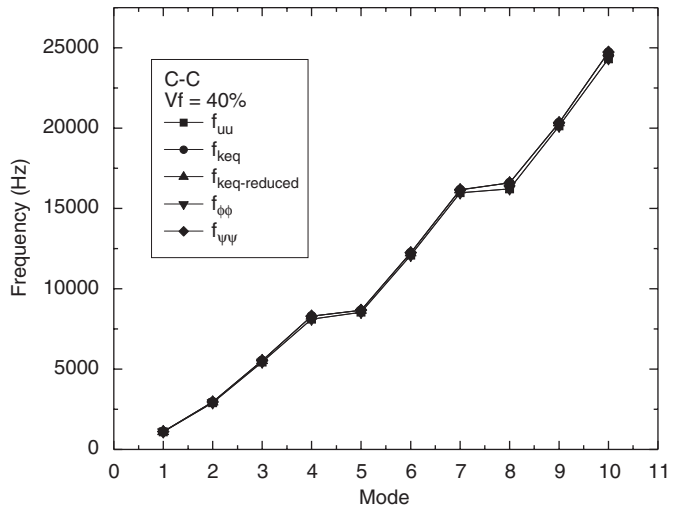

Fig. 9. Free vibrations of clamped–clamped multiphase MEE beam with vf = 40% $BaTiO_3$.

Fig. 6 shows the free vibration behaviour of vf = 40% $BaTiO_3$ beam, which consists 60% PM $CoFe_2O_4$, its influence on frequency of the structure due to magnetic effect is marginally higher when compared with the conventional structural frequency of beam. The graph of $f_{\phi\phi}$ coincides with the $f_{k_{eq}}$ graph. Fig. 7 shows the plot for vf = 80% $BaTiO_3$ beam, which consists only 20% PM $CoFe_2O_4$, its influence on frequency of the structure due to PE phase effect is marginally higher when compared with the conventional structural frequency of beam. At higher modes, the difference with system frequency and structural frequency is observed.

4.2.3. C– C beam

Tables 12–14 show the free vibration behaviour of multiphase MEE beam for vf = 0%, 60% and 100% of $BaTiO_3$, in $BaTiO_3$–$CoFe_2O_4$ composite for clamped–clamped end boundary conditions. For the study, $u = w = 0$ at both ends with $\psi = \phi = 0$ at ($x = 0$, $h/2$, and $x = L$, $h/2$). Table 12 shows the free vibration behaviour of vf = 0% $BaTiO_3$, which is purely a PM $CoFe_2O_4$, its influence on frequency of the structure due to magnetic effect is marginally higher when compared with the conventional structural frequency of beam. The $f_{\phi\phi}$ coincides with the structural frequency as the PE phase is absent for vf = 0% $BaTiO_3$. Similarly $f_{eq\_reduced}$ frequencies coincide with f_{eq} of the beam as the magnetoelectric effect is absent in single-phase beam.

Table 14 shows the free vibration behaviour of vf = 100% $BaTiO_3$, which is purely a PE $BaTiO_3$ its influence on frequency of the structure due to PE phase in the composite is higher when compared with the f_{uu} of beam. The $f_{\phi\phi}$ coincides with the $f_{k_{eq}}$ since PM phase is absent for vf = 100% $BaTiO_3$. Similarly $f_{eq\_reduced}$ frequencies coincide with f_{eq} of the beam as the magnetoelectric effect is absent in pure $BaTiO_3$ beam.

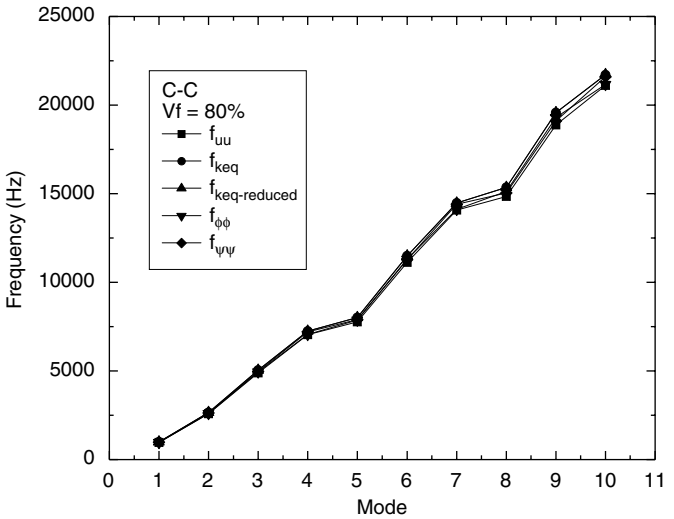

Fig. 10. Free vibrations of clamped–clamped multiphase MEE beam with vf = 80% $BaTiO_3$.

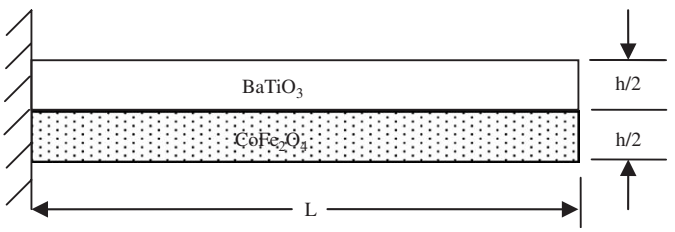

Fig. 11. Layered beam (B/F) for clamped–free boundary conditions.

Figs. 8–10 show the free vibration behaviour for vf = 20%, 40% and 80% vf of $BaTiO_3$, in $BaTiO_3$–$CoFe_2O_4$ composite for clamped–clamped beam. Fig. 5 shows the free vibration behaviour of vf = 20% $BaTiO_3$ beam, which consists 80% PM $CoFe_2O_4$, its influence on frequency of the structure due to magnetic effect is marginally higher when compared with the conventional structural frequency of beam. The graphs of all cases of frequencies overlap on each other indicating lesser influence. As the % vf $BaTiO_3$ increases in the $BaTiO_3$–$CoFe_2O_4$ composite, the PE and PM effect is observed for the beam at higher modes.

4.3. Layered beam

The free vibration studies on layered magneto-electro-elastic beam is carried out for two stacking sequences as B/F and F/B. The three boundary conditions C–C, S–S and C–F are studied. The study of layered beam is carried out by using Aboudi [9] material. The thickness of each layer in two layered beam is half the total thickness of beam. Here B represents 100% PE $BaTiO_3$ (vf = 100% $BaTiO_3$) and F represents 100% PM $CoFe_2O_4$ (vf = 0% $BaTiO_3$). Here B/F indicates a two layered beam with top layer is $BaTiO_3$ material and bottom layer of beam is $CoFe_2O_4$ material. Fig. 11 shows a two layered configuration.

4.3.1. Layered beam with C–F boundary condition

Tables 15 show the free vibration study for layered MEE beam (B/F) for clamped-free boundary conditions. Boundary conditions used for the study of layered magneto-electro-elastic beam are $u = w = \psi = \phi = 0$ at clamped end. The f_{uu} values for all the modes the beam coincides with $f_{\phi\phi}$. The values of $f_{k_{eq}}$ coincide with the $f_{eq\_reduced}$ and $f_{\psi\psi}$ frequencies. Magnetoelectric effect is not observed in the layered beam, with frequencies as $f_{k_{eq}}$ coincides with the values of $f_{eq\_reduced}$.

Fig. 12 shows the free vibration behaviour of layered MEE beam (F/B sequence) for clamped-free boundary conditions. The graph shows the increasing trend of frequencies as the mode number increase and the higher coupling effect on the free vibrations of beam at higher modes.

4.3.2. Layered beam with S–S boundary condition

The free vibration study for layered MEE beam (B/F and F/B) for simply supported boundary conditions. Boundary conditions used for the study of layered magneto-electro-elastic beam are $u = w = \psi = \phi = 0$ at $(x = 0,\ z = h/2)$ and $w = \psi = \phi = 0$ at $(x = L,\ z = h/2)$. Table 16 shows the free vibration behaviour of two layered beam with stacking sequence as B/F for simply supported beam. The f_{uu} values for all the modes the beam coincides with $f_{\phi\phi}$. The values of $f_{k_{eq}}$ coincides with the $f_{eq\_reduced}$ and $f_{\psi\psi}$ frequencies. No magnetoelectric effect is observed in the frequencies as $f_{k_{eq}}$ coincides with the values of $f_{eq\_reduced}$.

Table 15
Frequencies in Hz for clamped–free MEE layered beam (B/F)

Mode	f_{uu}	$f_{k_{eq}}$	$f_{k_{eq\_reduced}}$	$f_{\psi\psi}$	$f_{\phi\phi}$
1	188.68	188.70	188.70	188.70	188.68
2	1154.77	1154.65	1154.65	1154.65	1154.77
3	3122.07	3120.80	3120.80	3120.80	3122.07
4	4334.45	4335.11	4335.11	4335.11	4334.45
5	5842.88	5838.36	5838.36	5838.36	5842.88
6	9165.19	9154.66	9154.66	9154.66	9165.19
7	12944.50	12924.90	12924.90	12924.90	12944.50
8	12999.50	13001.50	13001.50	13001.50	12999.50
9	17068.10	17036.50	17036.50	17036.50	17068.10
10	21451.60	21405.10	21405.10	21405.10	21451.60

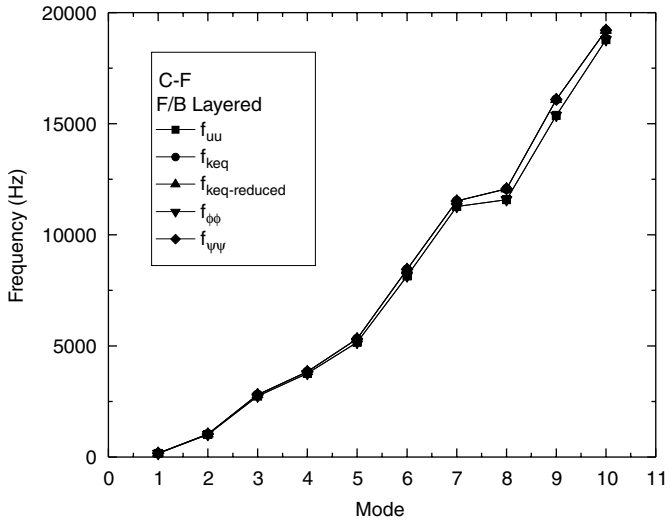

Fig. 12. Free vibrations of clamped–free F/B layered MEE beam.

Table 16
Frequencies in Hz for simply supported MEE layered beam (B/F)

Mode	f_{uu}	$f_{k_{eq}}$	$f_{k_{eq\_reduced}}$	$f_{\psi\psi}$	$f_{\phi\phi}$
1	526.26	526.29	526.29	526.29	526.26
2	2053.13	2052.71	2052.71	2052.71	2053.13
3	4010.34	4008.32	4008.32	4008.32	4010.34
4	4446.48	4444.36	4444.36	4444.36	4446.48
5	7536.74	7529.14	7529.14	7529.14	7536.74
6	11160.00	11146.30	11146.30	11146.30	11160.00
7	12057.90	12053.30	12053.30	12053.30	12057.90
8	15178.80	15150.10	15150.10	15150.10	15178.80
9	19487.00	19449.40	19449.40	19449.40	19487.00
10	20171.50	20163.40	20163.40	20163.40	20171.50

Fig. 13 shows the free vibration behaviour of two layered beam with F/B stacking sequence for simply supported beam. The values of modes of frequencies of f_{uu} coincides with values $f_{\psi\psi}$. The frequencies $f_{k_{eq}}$ coincides with the $f_{eq\_reduced}$ and $f_{\phi\phi}$ frequencies.

4.3.3. Layered beam with C– C boundary condition

Free vibration study for layered MEE beam (B/F and F/B) for clamped–clamped end boundary conditions is carried out with boundary conditions as $u = w = 0$ at both ends with $\psi = \phi = 0$ at ($x = 0$, $h/2$, and $x = L$, $h/2$). Table 17 shows the free vibration behaviour of two layered beam with stacking sequence as B/F. From the table it can be observed that the structural frequency of the MEE beam coincides with $f_{\phi\phi}$. The values of $f_{k_{eq}}$ coincides with the $f_{eq\_reduced}$ and $f_{\psi\psi}$ frequencies. No magnetoelectric effect is observed in the frequencies.

Fig. 14 shows the free vibration behaviour of two layered beam with F/B stacking sequence. The structural frequency of the beam coincides with $f_{\psi\psi}$. The values of $f_{k_{eq}}$ coincides with the $f_{eq\_reduced}$ and $f_{\phi\phi}$ frequencies.

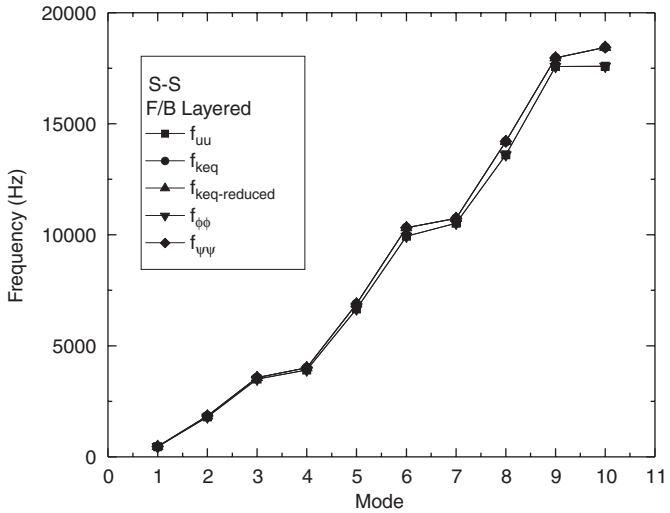

Fig. 13. Free vibrations of clamped–free F/B layered MEE beam.

Table 17
Frequencies in Hz for clamped–clamped MEE layered beam (B/F)

Mode	f_{uu}	$f_{k_{eq}}$	$f_{k_{eq\_reduced}}$	$f_{\psi\psi}$	$f_{\phi\phi}$
1	1165.34	1165.07	1165.07	1165.07	1165.34
2	3080.27	3078.60	3078.60	3078.60	3080.27
3	5744.55	5738.67	5738.67	5738.67	5744.55
4	8682.03	8683.41	8683.41	8683.41	8682.03
5	8983.76	8971.57	8971.57	8971.57	8983.76
6	12663.10	12640.40	12640.40	12640.40	12663.10
7	16677.80	16643.20	16643.20	16643.20	16677.80
8	17356.70	17358.00	17358.00	17358.00	17356.70
9	20951.10	20900.40	20900.40	20900.40	20951.10
10	25427.30	25360.00	25360.00	25360.00	25427.30

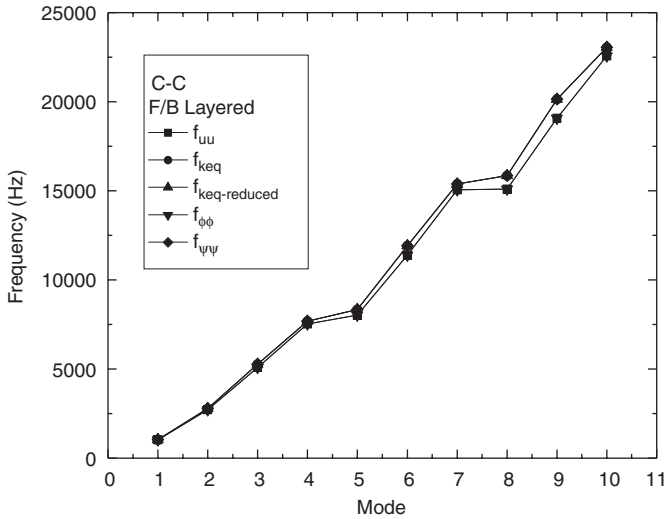

Fig. 14. Free vibrations of clamped–free F/B layered MEE beam.

5. Conclusions

1. Magneto-electro-elastic beam is modelled using four noded in-plane plate element.
2. The piezoelectric (PE) beam (vf = 100% $BaTiO_3$) is modelled in ANSYS for validation of frequencies with the code developed for three boundary conditions, i.e., C–C, S–S and C–F.
3. The free vibration study is carried out for multiphase and layered magneto-electro-elastic beam for three boundary conditions, i.e., C–C, S–S and C–F.
4. Three different magneto-electro-elastic materials are studied. It can be concluded that the effect of magnetoelectric constant is very minimal on the frequencies of beam.
5. The PE phase tends to increase the system frequency whereas the PM phase in multiphase beams tends to decrease the frequency behaviour.
6. The influence of PE and piezomagnetic (PM) phases is highest in clamped–clamped beams in comparison with clamped-free and simply supported beams. Since the stiffness of the beam in this configuration gives higher stiffness to the structure.
7. The stacking sequence has no much influence on the frequency behaviour of the layered beam but boundary conditions do show influence on the frequencies of the beam.
8. The study is useful in designing of smart sensors or actuators.

References

[1] C.-W. Nan, Magnetoelectric effect in composites of piezoelectric and piezomagnetic phases, *Physical Review B* 50 (1994) 6082–6088.
[2] D.A. Saravanos, P.R. Heyliger, Mechanics and computational models for laminated piezoelectric beams, plates and shells, *Applied Mechanical Review* 52 (1999) 305–320.
[3] T.-L. Wua, J.H. Huang, Closed-form solutions for the magnetoelectric coupling coefficients in fibrous composites with piezoelectric and piezomagnetic phases, *International Journal of Solids and Structures* 37 (2000) 2981–3009.
[4] E. Pan, Exact solution for simply supported and multilayered magneto-electro-elastic plates, *ASME Journal of Applied Mechanics* 68 (2001) 608–618.
[5] X. Wang, Z. Zhong, A finitely long circular cylindrical shell of piezoelectric/piezomagnetic composite under pressuring and temperature change, *International Journal of Engineering Science* 41 (2003) 2429–2445.
[6] E. Pan, P.R. Heyliger, Free vibrations of simply supported and multilayered magneto-electro-elastic plates, *Journal of Sound and Vibration* 252 (2002) 429–442.
[7] G.R. Buchanan, Free vibration of an infinite magneto-electro-elastic cylinder, *Journal of Sound and Vibration* 268 (2003) 413–426.
[8] A.R. Annigeri, N. Ganesan, S. Swarnamani, Free vibrations of clamped–clamped magneto-electro-elastic cylindrical shells, *Journal of Sound and Vibration* 292 (2006) 300–314.
[9] J. Aboudi, Micromechanical analysis of fully coupled electro-magneto-thermo-elastic multiphase composites, *Smart Materials and Structures* 10 (2001) 867–877.
[10] R. Buchanan George, Layered versus multiphase magneto-electro-elastic composites, *Composites Part B* 35 (2004) 413–420.
[11] A. Jiang, H. Ding, Analytical solutions to magneto-electro-elastic beams, *Structural Engineering and Mechanics* 18 (2004) 195–209.
[12] A.R. Annigeri, N. Ganesan, S. Swarnamani, Static studies on magneto-electro-elastic beam, *Proceedings of the ISSS 2005 International Conference on Smart Materials Structures and Systems*, Bangalore, July 2005.
[13] A.R. Annigeri, N. Ganesan, S. Swarnamani, Free vibration studies of simply supported layered and multiphase magneto-electro-elastic cylindrical shells, *Smart Materials and Structures* 15 (2006) 459–467.
[14] F. Ramirez, P.R. Heyliger, E. Pan, Free vibration response of two-dimensional magneto-electro-elastic laminated plates, *Journal of Sound and Vibration* 292 (2006) 626–644.
[15] F. Ramirez, P.R. Heyliger, E. Pan, et al., Static analysis of functionally graded elastic anisotropic plates using a discrete layer approach, *Composite Part B: Engineering* 37 (2006) 10–20.
[16] P.R. Heyliger, R. Fernando, E. Pan, Two-dimensional static fields in magneto-electro-elastic laminates, *Journal of Intelligent Materials Systems and Structures* 15 (2004) 689–709.
[17] A.K. Soh, J.X. Liu, On the constitutive equations of magnetoelectroelastic solids, *Journal of Intelligent Material Systems and Structures* 16 (2005) 597–602.